

단일주파수 CA코드 GPS 수신기를 이용한 CDGPS 정밀측위실험

원종훈, 고선준, 박현준, 이자성
아주대학교 전자공학부

Field Test Results of CDGPS Precision Positioning Using Single Frequency, CA Code GPS Receivers

Jong-Hoon Won, Sun-Jun Ko, Heun-Jun Park, and Ja-Sung Lee.
Division of Electronics Engineering, Ajou University.

Abstract - In this paper, field test results of a new efficient integer ambiguity resolution algorithm for precision Carrier Differential GPS(CDGPS) positioning are presented. The new algorithm is based on a reconfiguration Kalman filter which is designed to be used for the real-time precise positioning with low cost, single frequency, conventional C/A code GPS receivers. The tests were performed both in static and kinematic environment

1. Introduction

Precise positioning with GPS has been investigated in the surveying area where mm-level accuracy is required. This remarkable relative positioning accuracy is possible by using carrier phase measurements of GPS. To use carrier phase for positioning, however, initial integer ambiguity embedded in the carrier phase measurement must be resolved. For a short time span of data, numerous kinematic carrier phase ambiguity resolution techniques, called the On-The-Fly(OTF), which is the key to the real-time cm-level differential GPS positioning, have been proposed focusing on the improvement of the search speed and the reliability in the last several years. A carrier phase ambiguity resolution technique with static initialization was developed using high precision, single frequency, C/A code receivers and its end-products were put on market[1-3]. This technique was further enhanced to achieve the ambiguity resolution without static initialization[4,5]. In these works, the high code accuracy obtained from a specially dedicated high performance receiver equipped with a redundant narrow correlator technology is used to reduce the search space.

In order to apply the OTF algorithm for single frequency, C/A code receiver in real-time kinematic environment, it must work

- with single epoch L₁ frequency GPS data,
- without static initialization,
- with sufficiently fast computational speed and reliability,
- high output latency(1-20Hz).

Besides the conditions mentioned above, the carrier phase integer ambiguity resolution algorithm in low cost, single frequency, conventional C/A code receiver, which has the m-level code accuracy, has to overcome other problems: 1) Because the pseudorange measurements in conventional low cost C/A code receivers have m-level accuracy, the accuracy of float integer ambiguity solution is also degraded. The search space constructed from this level of observations is too big to be applicable in real-time integer ambiguity resolution because of its computational load and highly correlated covariance matrix. 2) The variation of the visible GPS satellites causes variations of ambiguity states in the filter.

In References 7 and 8, we developed a new OTF algorithm based on reconfiguration Kalman filter which overcomes the above mentioned problems while providing good performance improvement in a low cost, single frequency, conventional C/A code receiver. Computer simulation results are also presented in those references. In this paper, we verify its performance using actual field data.

2. Field Test Results

2.1 Test Environment and Equipments

The tests were performed on the top of the Engineering building at Ajou university, Suwon, Korea. In the static test, the antennas of the reference and the control point receivers were mounted with ground plane to minimize the effect of multipath error. In the kinematic test, a dom type antenna was used in the control point receiver. The GPS measurement data was obtained and stored by using two sets of precise survey purpose commercial GPS receivers, Trimble 4000ssi of Trimble Navigation Ltd.[6]. The reference receiver-computer set and antenna with ground plane are depicted in Figure 1 and 2, respectively, and the reference-control sites configurations are shown in Figure 3. The test environment and equipments are summarized in Table 1.

Table 1. Test environment and equipments

date/time	April 13th 2000, PM 4:00-6:00 (static) April 19th 2000, PM 1:00-5:00 (kinematic)
place	the roof of the engineering building, Ajou University, Suwon, Korea
test set	· GPS receiver (Trimble 4000ssi) 2 set · GPS antenna (ground plane/dom) 2 set -data update rate : 15 sec -data types : C1, P1, P2, L1, L2, D1, and D2* · reference station desktop computer (pentium, 200MHz) 1 set · rover notebook computer (pentium) 1 set

*C : C/A code, P : P code, L : carrier, D : doppler

For each of the antenna configurations, there are four baselines that were accurately determined by relative positioning with the commercial post-processing software package, GPSurveyTM of Trimble. The true ECEF coordinates of the each control point from this package are listed in Table 2. This control points were used as independent benchmarks to verify the quality of both static and kinematic solutions. The reference site is assumed to be at the origin of ENU coordinates, (0,0,0)(Table 2). In order to simulate a low cost, single frequency, C/A code GPS receiver, only the C/A code range(C1)

and the L_1 frequency carrier phase(L_1) are used in the algorithm among the seven measurement data, C1, P1, P2, L1, L2, D1, and D2, from the Trimble 4000ssi receiver. The accuracy level of the pseudorange from the receiver is m-level which is similar to that of conventional low cost C/A code receiver. Typical conventional C/A code receivers exhibit pseudorange measurement accuracy of a few meters(2 to 3 m) without S/A(The S/A operation has been removed since May 2000).

Table 2. The coordinates of reference and control points

	ECEF coordinates			ENU coordinates		
	X	Y	Z	E	N	U
reference:	-3060929.808	4055654.110	3842493.107	0.000	0.000	0.000
site A	-3060948.489	4055641.012	3842492.337	2.280	-1.097	0.694
site B	-3060953.952	4055647.386	3842481.044	23.322	-15.157	-0.005
site C	-3060993.728	4055615.957	3842482.601	74.004	-13.237	-0.044
site D	-3060988.060	4055609.407	3842493.526	73.343	0.690	-0.215

unit : meters

2.2 Static Tests

Figure 4 shows the a static test result at the control point D. It is shown in the figure that the number of the visible satellites is varied during the test run. The OTF based on the least-squares failed to resolve the correct integer ambiguity set because the search range from m-level pseudorange of conventional C/A code receiver is too large to search in a reasonable time span. It outputs the float solutions with m-level variance characteristics. In Kalman filter case, it continues to reduce the search range efficiently through prediction-correction procedure as time goes on and generates steady small variance float solution. The root-mean-squared errors of both algorithms at each control points are listed in Table 3. As shown in the table, the accuracy of Kalman filter is less than 30 cm. Figure 5 depicts the two dimensional positioning results of static test at each control points.

Table 3. Comparison of position error from the least-squares method and the Kalman filter in static test

	Least Squares	Kalman Filter
Site A	1.52	0.299
Site B	1.05	0.153
Site C	2.03	0.204
Site D	2.55	0.133

unit : m

2.3 Kinematic Tests

In the kinematic test, the rover moved around the pre-surveyed control sites(A→B→C→D). Figure 6 shows the roving receiver mounted on the back of a person who walks along the test path.

Figure 7 depicts the field test results in the kinematic case. The number of the visible satellites during the test run varied from 7 to 8. The result shows that the performance of the proposed filter is superior to the least-square method.

3. Conclusions

In this paper, a new real-time precise GPS positioning algorithm based on the reconfiguration Kalman filter has been tested and verified by processing the actual field data both in static and kinematic environment. All the double difference phase ambiguity estimates were identified in less than 2 minutes using the filter in all cases. The

result indicates that the state reconfiguration scheme performs efficiently in the situation where the number of visible satellites varies. It was verified that the new algorithm performs satisfactorily with noisy pseudorange data from conventional C/A code GPS receiver.

(References)

- [1] Lachapelle, G., Cannon, M.E., and Falkenberg, W., "High Precision C/A Code Technology For Rapid Static DGPS Surveys." *Proceedings of the 6th International Geodetic Symposium on Satellite Positioning*, Columbus, Ohio, Mar. 1992.
- [2] Ford, T. and Neumann, J., "Novatel's RT20 - A Real Time Floating Ambiguity Positioning System," *Proceedings of ION GPS'94*, The Institute of Navigation, Salt Lake City, UT, Sept. 1994, pp.1067-1076.
- [3] Masella, E., Gonthier, M. and Dumaine, M., "The RT-STAR: Features and Performance of A Low-Cost RTK OEM Sensor," *Proceedings of ION GPS'97*, Kansas City, MI, Sept. 1997, pp.53-59.
- [4] Cannon, M.E., Lachapelle, G., and Lu, G., "Ambiguity Resolution Without Static Initialization Using a High Performance C/A Code Receiver," *Proceeding of the 48th Annual Meeting*, The Institute of Navigation, 1992.
- [5] Cannon, M.E., Lachapelle, G., and Lu, G., "Kinematic Ambiguity Resolution with a High Precise C/A Code Receiver," *Journal of Surveying Engineering*, Amer. Soc. Civil Eng., Vol. 119, No. 4, Nov. 1993.
- [6] *GPSurvey Software User's Guide*, Trimble, Part Number 25749-00.
- [7] 원중훈, 고선준, 이자성, "재구성기법을 이용한 칼만필터 기반의 실시간 정밀 GPS 측위기법", 2000년도 대한전기학회 하계학술대회 논문집, 2000, 7, 17-20.
- [8] 이자성, 원중훈, 고선준, "방송파 위상차를 이용한 GPS 실시간 측지알고리즘 개발, 중소기업 기술혁신개발사업 위탁과제 최종보고서, 아주대학교 전자공학부, 2000. 3. 31.



Fig. 1. Reference receiver-computer set



Fig. 2. Reference antenna with ground plane at the roof of engineering building at Aju university, Suwon, Korea.

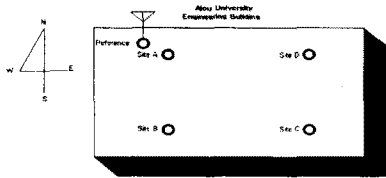
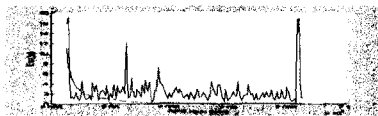


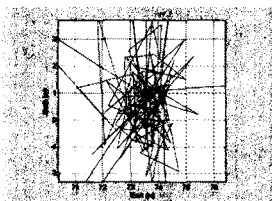
Fig. 3. Geometric configuration between reference and roving receiver sites



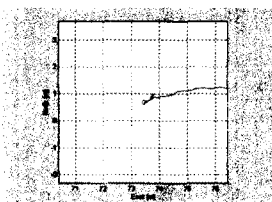
(a)



(b)



(c)



(d)

Fig. 4. Static field test result at site D

- (a) The variation of the number of the visible satellites
- (b) The comparison of the three dimensional positioning errors of the least-squares and Kalman filter
- (c) Two dimensional positioning output of least-squares
- (d) Two dimensional positioning output of Kalman filter

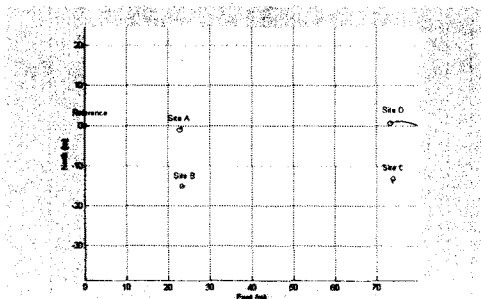


Fig. 5. Static field test results

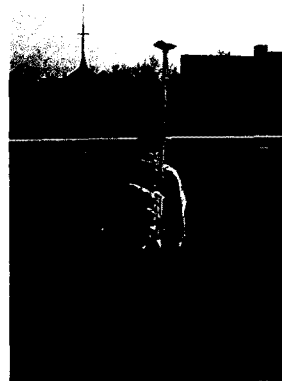
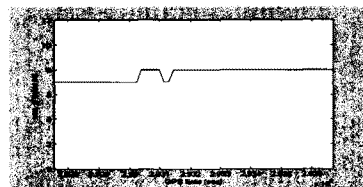
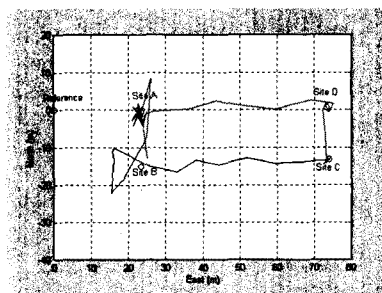


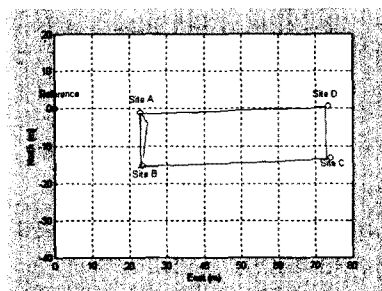
Fig. 6. Kinematic field test



(a)



(b)



(c)

Fig. 7. Kinematic field test results

- (a) The variation of the number of the visible satellites
- (b) Two dimensional positioning output of least-squares
- (c) Two dimensional positioning output of Kalman filter